Co-published by
Institute of Fluid-Flow Machinery
Polish Academy of Sciences
Committee on Thermodynamics and Combustion
Polish Academy of Sciences

http://www.imp.gda.pl/archives-of-thermodynamics/

Determination of the heat capacity of a water-ice reservoir as a lower heat source for heat pump - Numerical analysis

Piotr Tarnawski[a*]

[a]Warsaw University of Technology, Plac Politechniki 1, 00-661 Warsaw, Poland
*Corresponding author email: piotr.tarnawski@pw.edu.pl

Received: 10.10.2023; revised: 20.02.2024; accepted: 09.04.2024

Abstract

The paper presents the design of a heat exchanger immersed in a water-ice reservoir and the determination of its heat capacity as a lower heat source for the heat pump. This is an innovative solution, the first project on this scale in Poland. Heat absorption from the water-ice tank took place in three stages: from water at a temperature range of 20°C to 0°C, from the water-ice phase change at 0°C, and from ice at a temperature range of 0°C to –10°C. The CFD (Computational Fluid Dynamics) analysis of a heat exchanger performance was performed. It required simulation of water natural convection, water-ice phase change, and heat transfer from the ground. The heat flux absorbed in the designed exchanger was calculated based on the current glycol temperature and the implemented COP (Coefficient of Performance) characteristic of the heat pump. This was done via the user-defined function (UDF) available in Ansys FLUENT. The compiled internal software subroutine was defined based on the DEFINE_ADJUST macro. Moreover, the thermal resistance of ice forming on the pipes was included. The numerical analysis indicated that 66097 kWh of heat would be absorbed from the reservoir in 500 hours of exploitation. The volume fraction of water at the end of the simulation was equal to 26.7% and the volume fraction of ice was equal to 73.3%. The CFD simulation confirmed the heat capacity value of the water-ice storage tank which fulfilled the design requirements.

Keywords: Renewable energy; Water-ice tank; Ground reservoir; Heat pump; CFD simulation

Vol. 45(2024), No. 2, 157–163; doi: 10.24425/ather.2024.150862

Cite this manuscript as: Tarnawski, P. (2024). Determination of the heat capacity of a water-ice reservoir as a lower heat source for heat pump – Numerical analysis. *Archives of Thermodynamics*, 45(2), 157–163.

1. Introduction

One way to reduce fossil fuels for energy production is to use stored heat. The huge reservoir of stored heat is in the ground. Its average temperature is about 9 – 10°C [1,2]. This level of temperature makes it useful in the winter season for heating up and for cooling in the summer season. The most obvious way of using it is by heating and cooling ventilation air in an air-ground heat exchanger [3,4]. A more sophisticated approach is the use of the ground as a lower heat source for heat pumps [5,6]. The thermal energy of a tank filled with water as a storage medium gives better results because it has a greater heat capacity [7]. Water has a heat density of 1000 kg/m^3 and a specific heat capacity of 4200 J/(kg K). The ground density is 1750 kg/m^3 and its specific heat capacity is equal to 1200 J/(kg K).

Nomenclature

A – area, m^2
c – specific heat capacity, J/(kg K)
g – gravitational acceleration, m/s^2
h – sensible enthalpy, J/kg
H – enthalpy, J/kg
ΔH – latent heat content, J/kg
k – thermal conductivity, W/(m K)
L – latent heat of material, J/kg
p – pressure, Pa
$\dot{Q}$ – heat flux, W
q – density of heat flux, W/m^2
t – time, s
T – temperature, °C
S – source term (momentum sink), Pa
$\boldsymbol{w}$ – velocity vector, m/s

Greek symbols
β – liquid fraction
ε – momentum sink constant
μ – dynamic viscosity, Pa s
ρ – density, kg/m^3
$\boldsymbol{\tau}$ – stress tensor, Pa

Subscripts and Superscripts
HP – heat pump
mush – mushy zone
p – pull velocity

Abbreviations and Acronyms
2D, 3D – two-dimensional, three-dimensional
CFD – computational fluid dynamics
COP – coefficient of performance
PE – polyethylene
UDF – user-defined function

The water gives even more heat capacity when utilizing its phase changes during freezing and melting [8,9]. The heat of the phase change of water is equal to 333×10^3 kJ/m^3. In contrast, the heat capacity of liquid water is 4200 kJ/(m^3 K). The amount of latent heat accumulated in 1 m^3 of water during a phase change is equal to sensible heat accumulated in liquid water at the temperature of 80°C [10]. Heat absorbing from the water phase exchange proceeds at quite a low temperature which is equal to 0°C. But when it is used as a lower heat source for the heat pump it gives satisfactory results, since the temperature value is higher than external the temperature of the air in winter or the temperature of the ground around the pipes of the ground collector [5, 11]. As regards cooling purposes, a temperature of 0°C seems to be a very convenient temperature.

The paper presents a summary of the project focused on the design of a heat exchanger immersed in a ground water-ice tank and the determination of the thermal capacity of a tank. The water-ice reservoir is designed as an innovative lower-source solution for heat pumps in the system glycol/water. This system is designed to provide heat to public buildings of Science Center Cogiteon located in Cracow, Poland, as well as natural cooling in the summer, using clean and renewable energy sources.

The system consists of a special concrete tank filled with water. The heat pump absorbs energy from the tank using a heat exchanger made of many equally distributed polyethylene (PE) pipe loops. As heat is drawn from the tank, the water temperature drops until the freezing process begins. Additional energy, called phase change energy (latent heat), is released. Then the source (tank) can be regenerated using waste heat gained from the building. After the ice melts and the water temperature in the tank increases, the entire process starts again. This is an innovative solution, the first project on this scale in Poland.

The first chapter of the paper is focused on the tank construction and the design of a heat exchanger made of PE pipe loops. In the second chapter full description of the computational fluid dynamics (CFD) numerical approach is given. Then the most important results are shown and discussed. Finally, the results are concluded.

2. Design of tank heat exchanger

2.1. Aim of the analysis and its assumptions

The first goal of the project was to design a heat exchanger of a lower heat source (water-ice tank). The assumption for the project was that the exchanger should consist of 32×2 mm PE loop pipes. PE material is convenient since it can deform when water is freezing and melting. The length of a single-pipe loop should not exceed 100 m. The sum length of pipes of the heat exchanger shall be at least 7650 m. The working fluid was ethylene-glycol with a concentration of 35%.

The second goal of the project was to confirm by CFD simulation the assumed heat capacity of the water-ice tank. The amount of heat extracted from the tank must be at least 66000 kWh for the working period of 500 h. For purposes of the analysis, the heat pump has to work with a constant power of 200 kW. The heat pump should work with the parameters of the upper heat source as follows: inlet water temperature was equal to 35°C, and outlet water temperature of 45°C (supply temperature). The CFD simulation shall include changing the temperature of glycol in a lower heat source and changing the coefficient of performance (COP) characteristic of a heat pump.

2.2. Water-ice tank construction

The water-ice tank was made of concrete with a wall thickness equal to 0.5 m. It was located 6.7 m under the earth's surface. It had dimensions of 11.325 m×12.8 m×6.1 m according to Fig. 1.

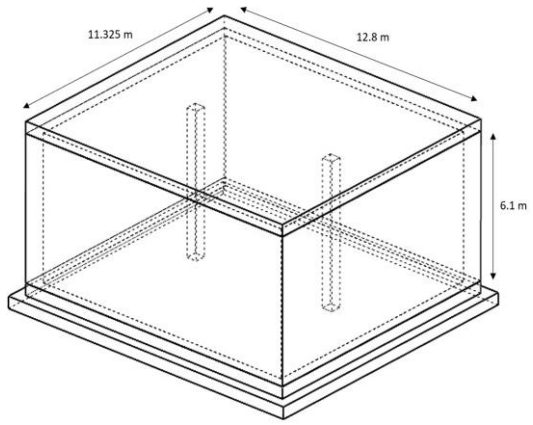

Fig. 1. Water-ice tank dimensions.

2.3. The arrangement of pipe loops in the water-ice tank

The minimum spacing between surrounding pipes should be 31 mm. It was calculated analytically based on that 712 m^3 of water has a latent heat equal to 66×10^3 kWh. To accommodate a heat exchanger with a total length of pipes equal to 7650 m, the pipes must be spaced every 31 mm.

From an operational point of view, the pipe loops should have the smallest possible pressure drop (the smaller the number of elbows the better). Moreover, the loops should have similar pressure drops (the same length and the same number of elbows), since they will be supplied from a common collector. The best solution is when pipe loops do not intersect each other. Figure 2 presents different considered variants of the arrangement of pipe loops. Each variant consists of 18 identical layers of pipe loops. The single layer consists of four pipe loops.

From a technical point of view, the best was VARIANT_4. It provided an equal length of pipe loops and the smallest pressure drop (only 56 elbows). In comparison, the VARIANT_2 had 136 elbows. See a comparison of the parameters of different arrangement variants in Table 1.

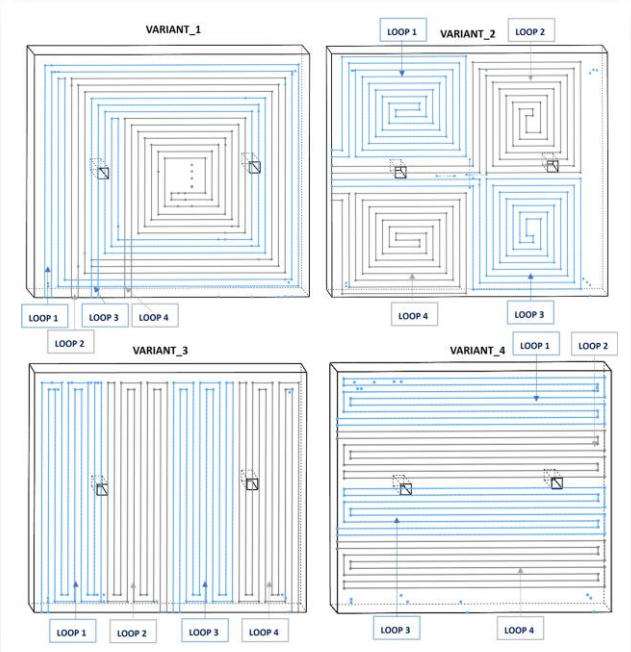

Fig. 2. Different variants of pipe loop arrangements in water-ice tank (single layers).

Table 1. Comparison of different arrangement variants of pipe loops.

VARIANT_1						
Loop	**1**	**2**	**3**	**4**	**Sum/ Layer**	**Sum /Tank**
Length [m]	105.4	108.5	105.4	106.9	426.1	7670
Elbows	10	12	14	28	64	

VARIANT_2						
Loop	**1**	**2**	**3**	**4**	**Sum/ Layer**	**Sum/ Tank**
Length [m]	98.5	105.2	98.5	105.2	407.4	7333
Elbows	34	34	34	28	136	

VARIANT_3						
Loop	**1**	**2**	**3**	**4**	**Sum/ Layer**	**Sum/ Tank**
Length [m]	106.8	106.8	106.8	106.8	427.2	7689
Elbows	18	18	18	18	72	

VARIANT_4						
Loop	**1**	**2**	**3**	**4**	**Sum/ Layer**	**Sum/ Tank**
Length [m]	100.2	100.2	100.2	100.2	400.9	7617
Elbows	14	14	14	14	56	

3. Description of CFD simulation approach

The CFD simulation had to include physics associated with laminar natural convection of water, freezing of water, and heat conduction in ice in transient mode. Moreover, the thermal interaction with the ground should be taken into account. It required resolving the equations of continuity, momentum, and energy, respectively:

$$\frac{\partial \rho}{\partial t} + \nabla \cdot (\rho \boldsymbol{w}) = 0, \tag{1}$$

$$\frac{\partial (\rho \boldsymbol{w})}{\partial t} + \nabla \cdot (\rho \boldsymbol{w}\boldsymbol{w}) = -\nabla p + \nabla \cdot \boldsymbol{\tau} + \rho g + S, \tag{2}$$

$$\frac{\partial (\rho H)}{\partial t} + \nabla \cdot (\rho \boldsymbol{w} H) = \nabla \cdot (k \nabla T), \tag{3}$$

where: ρ – density, t – time, $\boldsymbol{w}$ – velocity vector, p – pressure, $\boldsymbol{\tau}$ – stress tensor, g – gravitational acceleration, H – enthalpy, k – thermal conductivity, T – temperature, S – source term (momentum sink).

An enthalpy-porosity technique is used in Ansys FLUENT for modelling the solidification/melting process, based on the following equations [12]:

$$S = \frac{1-\beta}{\beta^3+\varepsilon} A_{mush}(\boldsymbol{w} - \boldsymbol{w}_p), \quad (4)$$

$$H = h - \Delta H, \quad (5)$$

$$\Delta H = \beta L, \quad (6)$$

where: β – liquid fraction, ε = 0.001 – constant, $A_{mush} = 10^5$ – default constant, h – sensible enthalpy, ΔH – latent heat content, L – latent heat of the material, $\boldsymbol{w}_p = 0$ – pull velocity.

In the enthalpy-porosity technique, the melt interface is not tracked explicitly. Instead, a quantity called the liquid fraction β, which indicates the fraction of the cell volume that is in liquid form, is associated with each cell in the domain. The liquid fraction is computed at each iteration, based on an enthalpy balance. The mushy zone is a region in which the liquid fraction β lies between 0 and 1. The mushy zone is modelled as a "pseudo" porous medium in which the porosity decreases from 1 to 0 as the material solidifies. When the material has fully solidified in a cell, the porosity becomes zero, hence the velocities also drop to zero. If $T < T_{solidus}$, $\beta = 0$; $T > T_{solidus}$, $\beta = 1$ [13,14].

The calculation of freezing is very time-consuming because for obtaining the solution convergence the single time step has to be very small [15,16]. For the assumed computation time step equal to 0.1 s and the required simulation period of 600 h, the two-dimensional (2D) simulation was only the option [17]. It was decided to simulate only a 2D repeating middle section of the tank heat exchanger which is shown in Fig. 4. However, such a 2D section should pretty well represent most of the tank region. The imperfection of the 2D approach was first of all, that it did not take into account the heat flux from the tank walls (only heat flux from the bottom of the tank was taken into account). It was a negligible simplification because as reported in the simulation, the amount of heat from the bottom of the tank was about 1% of the total heat absorbed from the tank. If the 2D model meets the requirements, the three-dimensional (3D) model will even better meet the requirements, because of additional heat from side walls [18]. The second simplification was that the 2D approach assumed a constant temperature of glycol, therefore, only a density of heat flux can be resolved. It is justified since the real temperature of glycol in a single pipe loop changes by only about 2 – 3 K [19]. After appropriate multiplication, the 2D solution can be used for the entire tank heat exchanger.

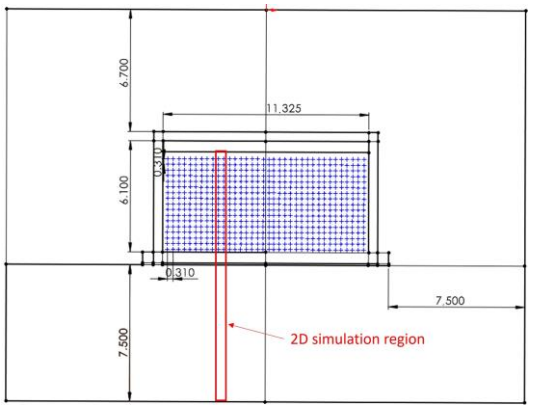

Fig. 3. Cross section of 3D model of the tank with surrounding ground.

The 2D geometry model, boundary condition, and computational mesh are shown in Fig. 3 and Fig. 4. The computational mesh consisted of quadrilateral elements with a total number of 12690. The smallest element in the vicinity of walls has a height equal to 1 mm. The thermal parameters of solids used in the simulation are shown in Table 2. The parameters of water and ice as a function of temperature are presented in Table 3. Changing the thermal parameters of water and ice in simulation allowed the current thermal resistance in the pipes' vicinity to be considered. The heat of the water-ice phase change (latent heat) was equal to L = 333 kJ/kg. The simulation took into account the real amount of water and the required mirror level of water. The analytical calculation included the sum of objects volume in the

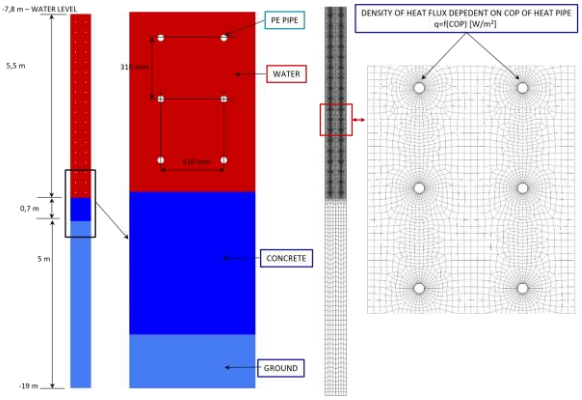

Fig. 4. A 2D simulation model of a tank heat exchanger with boundary conditions.

Table 2. Thermal parameters of solids used in simulation.

Material	Density ρ [kg/m³]	Thermal conductivity k [W/(m K)]	Specific heat capacity c [J/(kg K)]
PE	950	0.4	1750
Concrete	2500	1.7	840
Ground	1750	1.45	1200

Table 3. Parameters of water and ice in the function of temperature.

Temperature T [°C]	Density ρ [kg/m³]	Thermal conductivity k [W/(m K)]	Dynamic viscosity μ [Pa s]	Specific heat capacity c [J/(kg K)]
-20	919.4	2.39	-	1943
-15	919.4	2.34	-	1972
-10	918.9	2.30	-	2000
-5	917.5	2l25	-	2027
-0.05	916.2	2.22	-	2050
0.05	999.9	0.555	0.00175	4216
4.44	1000	0.566	0.00155	4204
10	999.7	0.589	0.0013	4195
15.6	999.2	0.609	0.00113	4187
21.1	998.1	0.625	0.00097 7	4183

tank (concrete poles, heat exchanger pipes, regenerating pipes, steel elements, others) and required free space in the upper part of the tank in a value of 10% of the water volume.

Figure 5 presents the COP change of the heat pump in function of glycol temperature. The supply temperature of water for this function was equal to 45°C. The lowest COP = 2.6 was for the temperature of glycol equal to –12°C. The highest COP = 5.5 was for the temperature of glycol equal to 20°C.

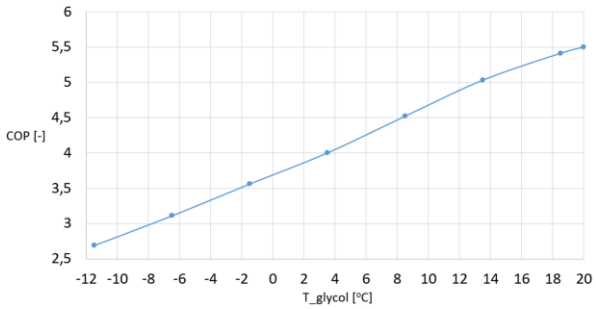

Fig. 5. COP characteristic of heat pump for supply water temperature of 45°C.

Thus, the heat flux absorbed from the water-ice tank should be calculated according to:

$$\dot{Q} = \dot{Q}_{HP} \cdot \frac{\dot{Q}_{HP}}{\mathrm{COP}(t)}, \tag{7}$$

where: $\dot{Q}_{HP}$= 200 kW – heat pump working power, COP(t) – COP function dependent on glycol temperature in pipes. See heat flux as a function of glycol temperature in Fig. 6.

The density of heat flux prescribed to the internal surface of pipes was calculated from:

$$q = \frac{\dot{Q}}{A}, \tag{8}$$

where A is the internal surface of the total pipe loops of the heat exchanger.

The calculation procedure required the use of advanced software UDF (user-defined function) capability. The compiled internal software subroutine was defined by DEFINE_ADJUST macro [17]. Within the subroutine, the temperature of the internal surface of pipe walls was read and averaged in each iteration. Next, using the COP function of the heat pump the new value of

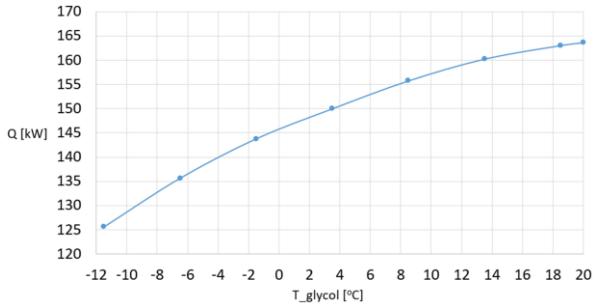

Fig. 6. Heat flux absorbed from the water-ice tank in the function of glycol temperature.

density of the heat source was prescribed to the internal surface of pipe walls. This procedure proceeded automatically over the simulated operating time of the tank heat exchanger. Simplification made in the analysis was that the temperature of glycol was assumed to be equal to the temperature of the inner surface of pipes. This is a reasonable assumption since the gradient temperature was below 0.05°C.

4. CFD simulation results

The initial temperature of the water was set to 20°C and the initial temperature of the ground was set to 8.9°C. While the heat was absorbed from the tank the water temperature dropped. It caused convection movements of water. The colder water was flowing to the lower part of the tank (Fig. 7). Below 4.44°C the flow direction has changed. The colder water was flowing to the upper part of the tank (Fig. 8). The reason for this was an increase in the density of water with a decrease in temperature from 21.1°C to 4.44°C, then a decrease in the density of ester with the change in temperature from 4.44°C to 0°C.

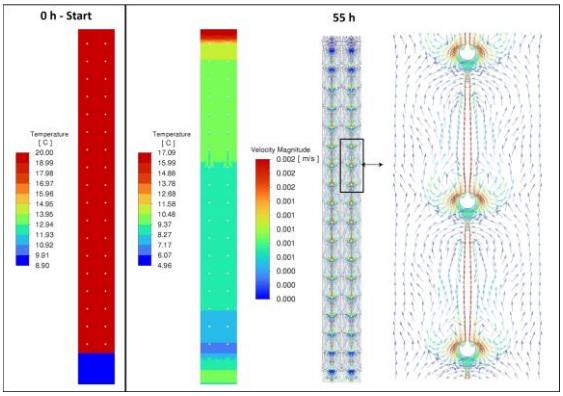

Fig. 7. Temperature and velocity distribution of water at the start and after 55 h of simulation.

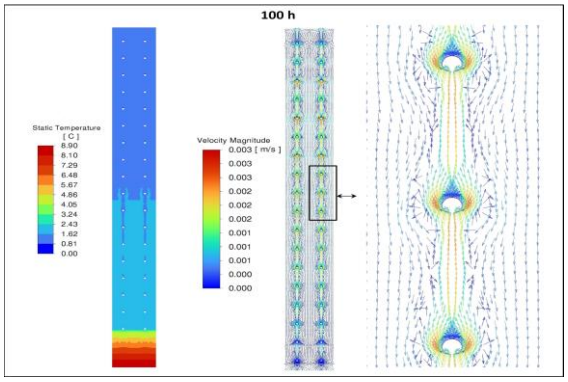

Fig. 8. Temperature and velocity distribution of water after 100 h of simulation.

When the water temperature reached 0°C the convective movements were stopped. The freezing process started firstly on the surfaces of the upper pipes (Fig. 9). The reason for this was

the flow of colder water to the upper part of the tank. The thickness of the ice around the pipes increased with the time of heat absorption (Fig. 10).

The simulation results indicated that 66097 kWh was absorbed in 500 h. After this time, the water volume fraction decreased to 26.7% and thus the volume ice fraction increased to 73.3%. As aforementioned, the simulation model included changes in water thermal properties in temperature function (Fig. 11). It allowed to take into account variable thermal resistance of the heat exchanger. An ice fraction of 98% was reached at 600 h after 86257 kWh of absorbed heat (Fig. 12).

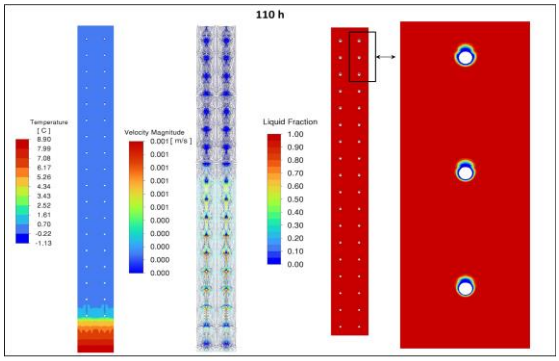

Fig. 9. Temperature, velocity, and liquid fraction distribution after 110 h of simulation.

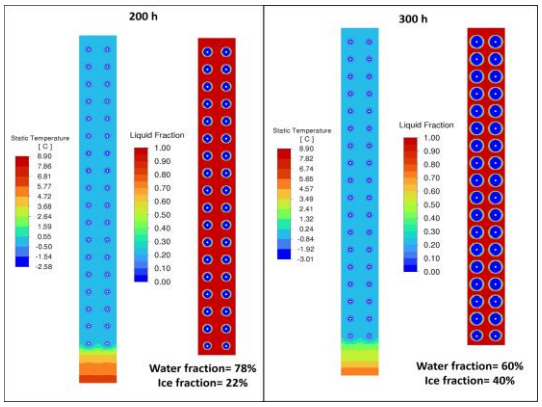

Fig. 10. Temperature and liquid fraction distribution after 200 h and after 300 h of simulation.

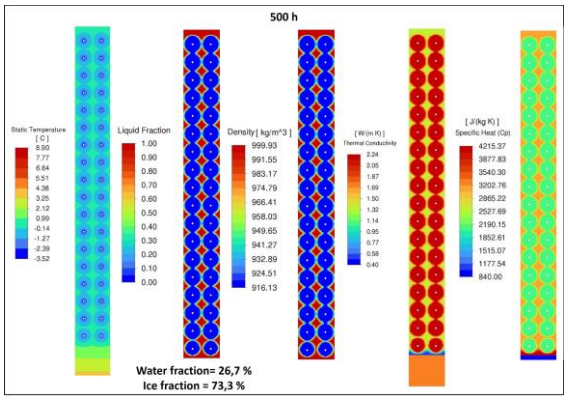

Fig. 11. Temperature, liquid fraction, and material properties distribution after 500 h of simulation.

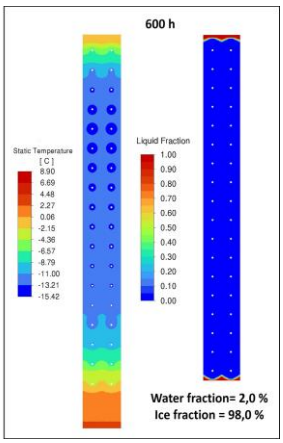

Fig. 12. Temperature and liquid fraction distribution after 600 h of simulation.

The change of glycol temperature throughout the simulation time of 600 h is presented in Fig. 13. As seen from the figure, the temperature decreased from 20°C to –10°C during convection and freezing. After reaching 100% of ice the temperature dropped below values acceptable by the heat pump. The smallest glycol possible working temperature was equal to –10°C.

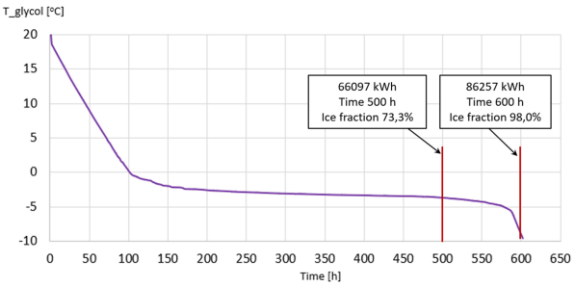

Fig. 13. Change of glycol temperature during heat absorption from water-ice tank.

The predicted heat flux absorbed from the tank changed according to Fig. 14. The maximum value was equal to 165 kW and the minimum value was equal to 130 kW at the end of the simulation.

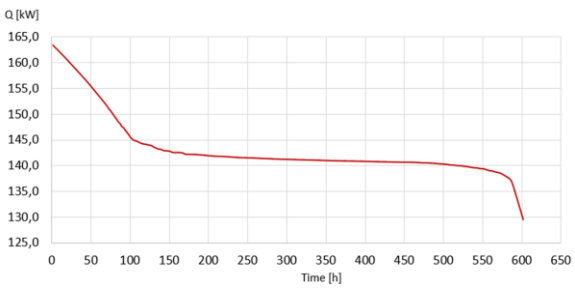

Fig. 14. Change in heat flux absorbed from the water-ice tank.

5. Conclusions

Several variants of pipe loops of the heat exchanger in a water-ice tank were considered and the optimal design was chosen for the CFD analysis. Then the simulation of heat absorption from the water-ice tank for 600 hours was carried out. The COP characteristic of the heat pump was taken into account as a function of the actual glycol temperature. Moreover, the thermal resistance of forming ice on the pipes of the heat exchanger was included. Such a procedure made it possible to take into account the actual amount of heat absorbed from the tank. As a result, the heat flux function absorbed from the tank throughout the entire working period of the heat exchanger was evaluated.

The simulation results showed that 66097 kWh of heat was absorbed from the water-ice tank during 500 hours. After this time the volume fraction of ice in the tank was equal to 73.3%, and the volume fraction of water was equal to 26.7%. This means that there was still a surplus of heat in the tank that could be further absorbed.

Assumptions on the heat capacity of the lower heat source (water-ice tank), as well as the adopted characteristics of the heat pump meet the requirements of the project. In the case of a real tank, the parameters should be better than in the simulation because:

1) The 2D simulation does not take into account the side walls of the tank from which the tank will be additionally heated (only the bottom of the tank is taken into account).

2) A conservative ground temperature of 8.9°C was assumed. When heating the tank to 20°C, the surrounding ground will also heat up, so its temperature will be higher than 8.9°C.

References

[1] Craciun, A. V., Sandu, F., & Pana, G. (2010). Monitoring of a ground source heat pump with horizontal collectors. In *12th International Conference on Optimization of Electrical and Electronic Equipment* (pp. 1–4). Brasov, Romania. doi: 10.1109/ OPTIM.2010.5510546

[2] Condego, P. M., Lorusso, C., De Giorgi, M. G., Marti, R., & D'Agostino, D. (2016). Horizontal air-ground heat exchanger performance and humidity simulation by computational fluid dynamic analysis. *Energies*, 9(11), 930. doi: 10.3390/en9110930

[3] Tarnawski, P. (2015). Analysis of the cooling performance of a tube ground heat exchanger. *Czasopismo Chłodnictwo i Klimatyzacja*, 8. (in Polish) http://www.chlodnictwoiklimatyzacja.pl/component/content/article/248-wydanie-08-2015/3609-analiza-cfd-wydajnosci-chlodzenia-rurowego-gwc.html [accessed: 18 Sep. 2023].

[4] Tarnawski, P. (2015). CFD analysis of ground heat exchanger performance. *Czasopismo Rynek Instalacyjny*, 6. (in Polish) https://www.rynekinstalacyjny.pl/artykul/projektowanie-c-o/20326,analiza-cfd-wydajnosci-rurowego-wymiennika-ciepla [accessed: 18 Sep. 2023].

[5] Hanuszkiewicz-Drapała, M. (2009). Modelling of thermal phenomena in ground heat exchangers of heating pumps, taking into account the flow resistance of the intermediary medium. *Modelowanie Inżynierskie,* 38, 57–68. ISSN 1896-771X (in Polish).

[6] Hanuszkiewicz-Drapała, M., & Bury, T. (2016). Utilization of the horizontal ground heat exchanger in the heating and cooling system of a residential building. *Archives of Thermodynamics*, 37(1), 47–72. doi: 10.1515/aoter-2016-0004

[7] Jastrzębski, P., & Saługa, P. (2018). Innovative methods of heat storage (in Polish). *Zeszyty Naukowe Instytutu Gospodarki Surowcami Mineralnymi i Energią Polskiej Akademii Nauk,* 105, 225–232. doi: 10.24425/124376

[8] Maślankiewicz, P., & Wojciechowski, H. (2017). Heating with freezing water. *Instal*, 4(2017), 19–23.

[9] Mania, T., & Kawa, J. (2015). Heat and cold energy storage systems – practical applications. *Energetyka,* 1 (in Polish).

[10] Jin, W., Suying, W., & Youtao, Z. (2010). Study on ice storage characteristics of a small-scale storage tank filled with ice balls. *Asia-Pacific Power and Energy Engineering Conference*. doi: 10.1109/APPEEC.2010.5448598

[11] Bezrodny, M., Prytula, N., & Tsvietkova, M. (2019). Efficiency of heat pump systems of air conditioning for removing excessive moisture. *Archives of Thermodynamics*, 40(2), 151–165. doi: 10.24425/ather.2019.129546

[12] ANSYS. (2018). *Fluent Theory Guide 19.1, Chapter 18: Solidification and Melting*.

[13] ANSYS® Academic Associate CFD. *ANSYS Fluent User Guide.*

[14] Selvenes, H., Allouche, Y., Sevault, A., & Hafner, A. (2019). CFD modeling of ice formation and melting in horizontally cooled and heated plates. In *Eurotherm Seminar 112: Advances in Thermal Energy Storage*, 15–17 May, Lleida, Spain.

[15] Ramesh, V., Terala, S., Mazumder, S., Matharu, G., Vaishnv, D., & Ali, S. (2021). Development and validation of a model for efficient simulation of freezing of water in large tanks. *Journal of Thermal Science and Engineering Applications*, 13(1), 011008. doi: 10.1115/1.4047166

[16] Ramesh, V., Terala, S., Mazumder, S., Matharu, G., Vaishnv, D., & Ali, S. (2022). Efficient simulation of freezing of water in large tanks including expansion of ice. *Journal of Thermal Science and Engineering Applications*, 14(11), 111006. doi: 10.1115/1.4054513

[17] Michałek, T., & Kowalewski, T. (2003). Simulations of the water freezing process – numerical benchmarks. *Task Quarterly*, 7(3), 389–408.

[18] Muszyński, T., & Kozieł, S. M. (2016). Archives of thermodynamics. *Archives of Thermodynamics*, 37(3), 45–62. doi: 10.1515/aoter-2016-0019

[19] Hanuszkiewicz-Drapała, M., & Składzień, J. (2010). Heating system with vapor compressor heat pump and vertical U-tube ground heat exchanger. *Archives of Thermodynamics*, 31(4), 93–110. doi: 10.2478/v10173-010-0031-8